



An appraisal of the sedimentation pattern and age profile of Perumal Lake, using radiometric analysis of ^{210}Pb and ^{137}Cs tracers

Vasudevan Sivaprakasam¹ · Baranidharan Sathyanarayanan¹ · V. Vijayakumar¹ · Sivaranjan Periyasami¹ · Pravinraj Sambath¹

Received: 13 March 2024 / Accepted: 7 August 2024 / Published online: 22 August 2024
© The Author(s), under exclusive licence to Springer-Verlag GmbH Germany, part of Springer Nature 2024

Abstract

This present investigation delves into the intricate ^{210}Pb and ^{137}Cs radionuclides dating to govern the study of sedimentation rate, age modeling, and lifespan of the Perumal lake in the Cuddalore district, Tamil Nadu. In the study area, the 01 core sediment was excavated at the length of 51 cm, and concern for the ^{210}Pb and ^{137}Cs radionuclides dating using an Alpha spectrometer 7200-04 and a Gamma-ray spectrometer GC-3520 instruments. From the robust outcome, the bathymetry survey investigates the bottom topography, with a mean depth of 3.1 m and a maximum length of 11.54 km. Subsequently, the mean value of bulk density, porosity, and water content in the vertical profile of the sediment esteems as 1.52 g/cm³, 32.47 g/cm³, and 1.61%, and sediment textures unveils predominately consists of clay composition and attributes with higher content of ^{210}Pb radionuclide in the sediments to affirms the rate and accumulation of the sediments in the aquatic environment. From the Constant Rate Supply (CRS) method, the ^{210}Pb radionuclide activity shows the mean accumulation rate (kg/m²/year) and sedimentation rate (cm/year) indicates 0.57 ± 0.05 (kg/m²/year) and 0.84 ± 0.07 (cm/year) dated since 1944AD to 2023AD. The mean sedimentation rate of ^{137}Cs radionuclides activity for 1963AD and 1986AD implies 0.57 ± 0.04 (cm/year) and 0.43 ± 0.03 (cm/year). From the computation, the lifespan of the lake is 369.05 years and 543.86 years with respect to ^{210}Pb and ^{137}Cs activities, respectively. The sedimentation rate is crucial in diminishing the lake from the future accumulation of water and sediments in the aquatic environments.

Keywords Sediment textures · ^{210}Pb and ^{137}Cs radionuclides dating · Wetland lifespan · Perumal Lake

Introduction

Wetlands/Lakes contribute to water requirements for local residences and agricultural and industrial activities worldwide, and they are considered the kidneys of the landscapes. River, rainwater, brackish, and glacial meltwater are essential lake water sources (Fairbridge 1968). The wetland accumulates with the sediments regularly via streams, rivers, and entering overland flow. Aggregation of the sediments in the plain region of the lake's environs depends on the slope, vegetation cover, and geology of the lake catchments. On the lake floor, the sediment deposits happen slowly as a natural process, reducing storage capacity light penetration, encouraging biotic growth, and affecting the ecosystem's

functioning. Elevated anthropogenic activities in recent years have affected the hydrological regime of lakes in the country (Singh et al. 2008). Almost 12% of the global human population lives in the mountain regions (Das and Vasudevan 2021). At altitudes above 3500 m Mean Sea Level (MSL), the wetlands formed due to the glacial meltwater and are defined as "glacial wetlands" (WWF 2005). The wetland in the high altitude regions experiences high input of sediment loads due to the steep inclines and transportation of dissolved materials due to water, occasional variation in the diverse plant canopy, and later formative exercises (Das et al. 1994; Diwate et al. 2020). At high altitudes, Himalayan wetlands indicate an enormous input of sediments that diminish the lake environments. The higher sediment inputs and lithological vulnerability are mainly worth noticing in the variation of high altitude Himalayan Lake (Kothari 1996; Kumar 1999a, 1999b; Rai 2007b; Singh 2007; Singh et al. 2008; Humane et al. 2016). Many researchers have investigated the wetlands sedimentation rate and deposition

✉ Vasudevan Sivaprakasam
devansiva@gmail.com

¹ Department of Earth Sciences, Annamalai University, Annamalai Nagar, Chidambaram, Tamil Nadu 608002, India

characteristics (Kusumgar et al. 1989; Das et al. 1994; Kumar et al. 1999c; Das and Vasudevan 2021; Singh and Vasudevan 2021; Rout and Vasudevan 2022; Palani et al. 2023; Guan et al. 2023; 2024). In the wetlands, the enormous input of the sediments deciphers the death of the lake environments (Mondal et al. 2012; Nautiyal et al. 2012; Chandrakiran and Kuldeep 2013; Khadka and Ramanathan 2013; Bhat and Pandit 2014). The insights of the present study will support erosion control, sediment impediment, and future lake management strategies.

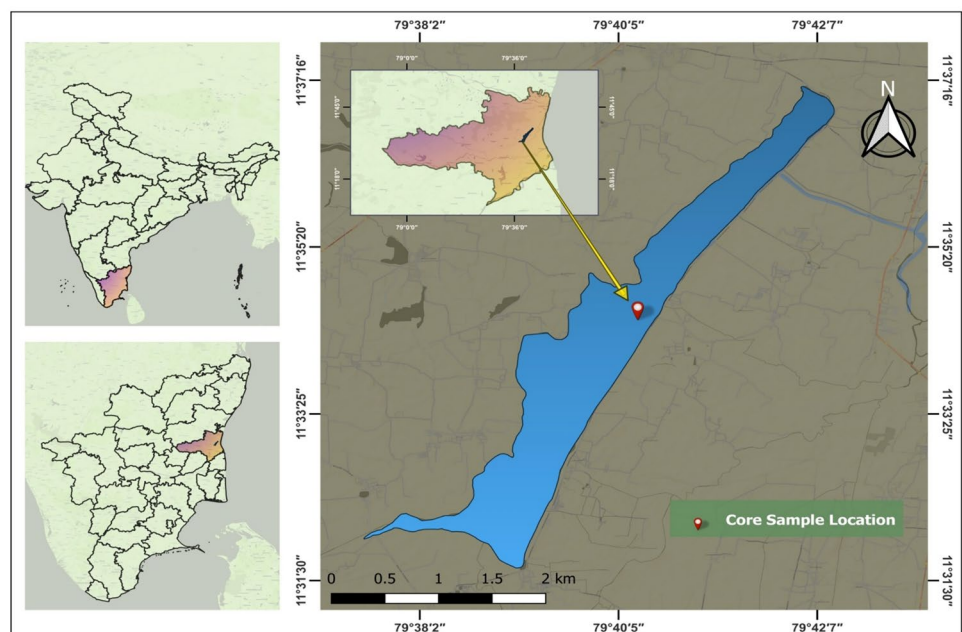
The radioisotopes from natural and artificial sources can be found in lake sediments. To estimate the sedimentation rate, the radioisotopes ^{210}Pb (Lead-210) and ^{137}Cs (Cesium-137) have been particularly helpful in dating the sediment deposit in lakes and reservoirs. Out of all the radioisotopes, the ^{210}Pb and ^{137}Cs activities occur naturally and artificially in the aquatic environment (Ritchie and McHenry 1990; Edington et al. 1991; Kumar et al. 2007; Semertzidou et al. 2019; Singh and Vasudevan 2021). Natural radionuclide ^{210}Pb and anthropogenic ^{137}Cs were used to estimate the current sedimentation rate in lake environs (Edington et al. 1991; Putyrskaya et al. 2020; Strakhovenko et al. 2020). It is worth noticing the ^{210}Pb activities for evaluating wetlands sedimentation rates and unveiling the chronological age of the lakes. The half-life of the ^{210}Pb indicates 22.20 ± 0.17 years (Goldberg 1963) due to ^{226}Ra (Radium-226) decay in the sediments, resulting from the ^{238}U (Uranium-238) decay chains. Calculate the sedimentation rates over 120–150 years using the ^{210}Pb radionuclide sources (Corcoran et al. 2018). A significant quantity of the artificial radionuclide ^{137}Cs was presented in 1963, primarily due to atmospheric fallout from thermonuclear weapon

tests during the 1950s and 1960s (UNSCEAR 2000). Several incidents, such as the Chornobyl Accident (CA) disaster on April 26, 1986 (Appleby 2001; Shah et al. 2020), and the Fukushima Daiichi Nuclear Power Plant (FNPP) incident on March 11, 2011 (Butler 2011; Chino et al. 2011), have led to the enrichment of ^{137}Cs radionuclides in the environment. The artificial radionuclide ^{137}Cs served as a validation tool for analyzing ^{210}Pb natural radionuclides in establishing temporal sedimentation rates and age models for wetland environments (Appleby 2001; Guo et al. 2020). This present study focuses on evaluating the status of the sedimentation rate and age model for Perumal Lake along with life computation, which can identify the influences of the rate of depositions on appropriate management of the wetland environments.

Description of study area

The present study investigates Lake Perumal, near the Neyveli lignite mines in the Cuddalore district. Intriguingly, the lake describes narrow elongated southeast slopes, and it is an artificial lake roost at an altitude above the 24.38 m MSL. The profound study of the lake argues that it is a closed basin with admissibly 13.24 sq. km and is situated east of the Neyveli lignite mines. It has significant input from the Neyveli lignite mining regions through the Paravanar River and lies between north latitudes $11^{\circ} 30'$ to $11^{\circ} 45'$ N and East longitudes $79^{\circ} 30'$ to $79^{\circ} 47'30''$ E (Fig. 1). The physiography of Lake Perumal demonstrates the area is almost a plain coastal area, and river alluviums exist on most of its part with slightly high ground of Tertiary sediments

Fig. 1 Sample location map of core sediment of the Perumal Lake



followed by geographic features of the study reveal Gadilam and Ponnaiyar rivers in the north, and Vellar and Coleroon river in the south drains to the lake. Subsequently, the morphometric characteristics of the lake represent the undulate bottom floor with a maximum water depth of 5.6 m recorded in the northeastern part of the surveyed area of the water body (Table 1).

Materials and methods

Bathymetry forecast

Evaluating the bathymetry of a lake basin is crucial for assessing the lake's condition and comprehending its management prospects and stipulations. A Garmin GPS Map 178 (Chartplotter/Sounder) was equipped with a dual-frequency 50/200 kHz transducer, providing a 10-cm vertical accuracy within the 120-degree and 450-degree cone angles. The transducer is fitted on the back of the boat, the Global Navigation Satellite System (GNSS) receiver external antenna is mounted above the transducer, and the displaying unit is positioned on the front side of the boat (Szarlowicz et al. 2017). Forty-eight bathymetric data points were rigorously collected, along with their corresponding paths and locations. The bathymetric points were accurately acquired using a GNSS receiver to determine the lake's depth and then imported into ArcGIS 10.8.2 software for analysis. In the bathymetric modeling process, inverse distance weighting (IDW) interpolation was employed to anticipate measured depths from adjacent locations to estimate depths at unknown points (Bedient and Huber 1992; Burrough and McDonnell 1998).

Core sampling and analysis

On March 2023, the one core sediment was reclaimed at a depth of 5.0 m and was chosen based on a bathymetry

Table 1 Data represents the morphometric parameters of Lake Perumal

Morphometric parameter	Morphometric value
Area	13.24 km ²
Shoreline length	31.61 km
Shore development index	2.45
Maximum length	11.54 km
Maximum width	2.07 km
Mean width	1.14 km
Maximum depth	5.6 m
Volume	41,044 m ³
Mean depth	3.1 m
Direction of the major axis	NE–SW

map from the center part of the closed basin at the geo-coordinates (latitude $-11^{\circ}34'30''$ N & longitude $-79^{\circ}40'20''$ E) of the Perumal Lake employs the gravity coring method. Temporal core sediment recovered with a diameter of 58 mm, followed by a length of 51 cm. The retrieved core was securely packed and kept in a vertical orientation during sampling to prevent any disturbance to the sediment within the coring tube. To avoid sediment compaction during transportation, proper precautions include keeping the containers stable and upright, avoiding excessive shaking or jolting during transport, using appropriate cushioning material to minimize movement, and securing the samples to maintain their original structure. The core sediment was safely transported to the laboratory for further analysis.

The core sediments were stored in the freezer at $+4^{\circ}\text{C}$ for seven days before sub-sampling into 1 cm intervals (Gharibreza et al. 2013). To remove the moisture content, the sediment samples were subjected to a hot-air oven to dry at 70°C for 12 h (Sert et al. 2016). The quantification of dried samples was determined to concede the bulk density, and the dry weight sample helps us achieve the water content based on the calculated weight reduction of dry samples subtracted from the wet samples. Sediment samples were dried before calculating the percentage volume of water in the pores relative to the total volume of sliced core sediment samples (Das and Vasudevan 2021; Palani et al. 2023). The sediment samples were again heated at 60°C for about 24 h to remove the moisture content in the hot air oven. Dry sediment samples were gently crushed by using agate mortar at a grain size $<200\ \mu\text{m}$ and were homogenous. The sediment samples were utilized for subsequent analyses, including assessments of grain size distribution and identifying radioactive nuclides as part of further investigations.

The grain size analysis was performed with the Horiba LA-300 Scattering particle size analyzer. The sediment samples were preprocessed by the double distilled water + hydrogen peroxide (H_2O_2) with a ratio of 1:1 and Double distilled water + hydrochloric acid (HCl) with a ratio of 2:1 to decrease the effects of soluble salts, organic matters, and carbon contents. Additionally, at the time of analysis, a pinch of Sodium hexametaphosphate (NaPO_3) was added to separate the fine sediments from the bonding of the particles (Singh and Vasudevan 2021; Palani et al. 2021, 2023). The anticipated outcomes were standardized using the Wentworth scale method to determine the sediment fractions (Wentworth 1922).

To appraise the ^{210}Pb and ^{137}Cs radioactivity using the α and γ spectrum analyzing system assists in the Analytical Chemistry Division, Bhabha Atomic Research Centre (BARC), Trombay, Mumbai, India. From the 01 g of powdered sediment samples, the radiochemical separation of ^{210}Po was digested using a closed microwave digested system (Milestone Srl, Model Ethos, and Italy) pricked

with ^{209}Po tracers, and HF: HNO_3 (1:1) as well as hydrogen peroxide (H_2O_2) in Teflon beakers as per the guidelines in the manual from the manufacturer. To reduce the Fe, add ascorbic acid to convert Fe^{3+} to Fe^{2+} with the aid of ^{210}Po and ^{209}Po mounted in the silver planchets along with 0.5 N HCl solutions at 90 °C for three hours. ^{210}Po activity was estimated with alpha energy of 5.30 MeV using ^{209}Po (4.88 MeV alpha emission) as the internal tracer by alpha spectrometry (ORTEC, OCTAT) with 13% efficiency, 20 keV resolutions, and 300 mm² areas with a depletion depth of 100 nm. Intercalibration exercises were also performed using standard samples (IAEA-414). Blanks were run through the same analytical procedures as samples to ensure no contamination from analytical reagents. Afterward, meticulous observation was carried out on ^{210}Pb activities were determined from its granddaughter (^{210}Po) with alpha spectrometry during the secular equilibrium stage (Wood et al. 1997; Sanchez-Cabeza et al. 1998; Henderson et al. 1999; Al-Masri et al. 2003; San Miguel et al. 2004). Each segmented samples were counted ranging from 6×10^4 to 8×10^4 s, although the background value was accounted for and calculated for every five samples for the time interval of 2×10^4 to 3×10^4 s. The formula adopted to evaluate the specific activity (Bq/g) of the measured ^{210}Po radionuclide through its marked ROI (Region of Interest) and activity counts. The formula has been mentioned below as,

$$\text{Specific activity} \left(\frac{\text{Bq}}{\text{g}} \right) = \left(\frac{\text{Counts}}{\text{Time(s)}} - \frac{\text{Bkg Counts}}{\text{Time(s)}} \right) \times \frac{100}{\text{Efficiency(\%)}} \times \frac{1000}{\text{Sample Weight(g)}} \quad (1)$$

where Bkg stands for background counts of polonium measured as 0.025cps, which is 2000 counts in 80,000 s; 13% efficiency, 2 g of sediment weight. The $^{210}\text{Pb}_{\text{sup}}$ (^{210}Pb —supported) activity was assessed as the mean of assorted constant $^{210}\text{Pb}_{\text{exc}}$ (^{210}Pb —unsupported) determination in the bottom sediment layers (beneath the zone of $^{210}\text{Pb}_{\text{exc}}$ exponential decline) (Zaborska et al. 2007). The $^{210}\text{Pb}_{\text{exc}}$ was estimated by subtracting the total ^{210}Pb activity and $^{210}\text{Pb}_{\text{sup}}$, which are in secular equilibrium (Appleby and Oldfield 1992).

To manage the ^{137}Cs activities using gamma spectroscopy aided with a well-type NaI (TI) crystal detector with the size of 4" × 4" a well of 1" diameter × 2" height. Each sample was counted for 6×10^4 to 8×10^4 s for gamma counting. For a period of 2×10^4 to 3×10^4 s, the background (Bkg) values were recorded using intervals of 10 samples. The concentration of ^{137}Cs was dictated by estimating the gamma peak at 661.62 keV with an 85% branching ratio. The lower limitation of detection, with 95% confidence, was 0.3 Bq for 24 h of measuring time. The energy calibration of the instrument

was done with a mixture of ^{137}Cs and ^{60}Co sources, and the efficiency calibration was done with reference standard soil (IAEA-326) (Singhal et al. 2012) for the quality control of the gamma spectrometer. Reference and repeated samples showed ^{137}Cs values in an acceptable range of activity (Kumar et al. 2008; Gharibreza et al. 2013). The formula was adopted to evaluate the specific activity (Bq/kg) of the measured ^{137}Cs radionuclide of each sample with the aid of gamma counting.

$$\text{Specific activity} \left(\frac{\text{Bq}}{\text{g}} \right) = \left(\frac{\text{Counts}}{\text{Time(s)}} - \frac{\text{Bkg Counts}}{\text{Time(s)}} \right) \times \frac{100}{\text{Gamma Abundance}} \times \frac{100}{\text{Efficiency(\%)}} \times \frac{1000}{\text{Sample Weight(g)}} \quad (2)$$

where Gamma abundance is 85.1, efficiency is 31.94%, and the background value in cps was 0.006 (480 counts in 80,000 s).

Chronology of age-depth sedimentation model

^{210}Pb radionuclide models

The sedimentation model shows positive results in building the chronological or age depth of the sediment deposition in the wetlands. The sedimentation model has two dating approaches to decipher the chronological or age-depth. Two models are named Constant Rate Supply (CRS) and Constant Initial Concentration (CIC) (Appleby and Oldfield 1978; Robbins et al. 1978). The (CIC) model is unsuitable for this study's criteria due to the constant rate of accumulation accompanied by a repeatedly diminishing abundance of ^{210}Pb (Alhajji et al. 2014).

According to Krishnaswamy et al. (1971) put forth the CRS model to assess the sedimentation rate and age-depth of the core sediments with the steady ^{210}Pb fallout from the atmosphere to the ocean or lake water at the consistent rate of supply of ^{210}Pb to the sediments. The CRS model addresses an oscillation in sediment supply while adopting a ^{210}Pb flux configuration. The outcome of the CRS model indicates that many sedimentary basins and sediments fluctuate due to climate or human-induced alterations. The cumulative residual $^{210}\text{Pb}_{\text{exc}}$, A_d , beneath deposits of age t varies concerning the formula.

$$A_d = A_0 e^{-\lambda t} \quad (3)$$

where, $t=x/s$

So,

$$s = x/t \quad (4)$$

(Liang Kangkang et al. 2014).

where the A_d defines unsupported ^{210}Pb in the temporal sediments below the depth " d ," and A_0 is the entire unsupported ^{210}Pb below the mud/water interface (Gharibreza et al. 2013), S is the rate of sedimentation, x indicates the depth of the sediment deposits, and t infers estimated time (year).

The sediment's age at any depth can be calculated using the below-given formulae,

$$t = \frac{1}{\lambda} (\ln A(0)/(d)) \quad (5)$$

Using a temporal sediment sample from Perumal wetlands, the model's applicability was entirely investigated.

^{137}Cs radionuclide model

Notably, the ^{137}Cs activity spiked in 1963, which is considered a key marker year (Albrecht et al. 1998) due to the Nuclear Test Ban Treaty. In the following years, the ^{137}Cs spike rate decreased sharply and is scarcely accountable because of lower atmospheric ^{137}Cs concentration. Additionally, the ^{137}Cs peaked in 1986 may be due to the effect of the Chernobyl accident, also considered a key marker year (Palani et al. 2023; Rout and Vasudevan 2022; Das and Vasudevan 2021; Singh and Vasudevan 2021). The profound study of ^{137}Cs activity peak variations (i.e., increase or decrease) in the depth profile did not affect the heightened area of the concentration or time marker zone (Zapata 2002; Zhang et al. 2012; Cheng et al. 2019). The formula to derive the sedimentation rate is estimated as follows,

$$r = \frac{H}{(n - Y)} \quad (6)$$

where r value unveils the sedimentation rate (cm/year) for this samples, H is denoted as the depth (cm) of the Key marker year Y (1963 or 1986) of ^{137}Cs activity peak, and followed by n infers the sampling year i.e., 2023. As well as the age of the excavated core sediments above deposited respective Key marker year (1963 or 1986) depth can be defined as,

$$T_n = Y + ((H - h_n)|r) \quad (7)$$

Above the marker year (Cheng et al. 2019).

The formula for the sediment layer deposited below the respective key marker year (1963 or 1986) is calculated as,

$$T_o = Y - ((h_o - H)|r) \quad (8)$$

Below the marker year (Cheng et al. 2019).

where, Y is the marker year; T_n and T_o are the age (year) above and below the key marker year; and h_n and h_o are denoted as depth (cm) for these layers, respectively. The

accuracy of ^{210}Pb dates via the CRS model is substantiated by reference to the well-determined peaks of ^{137}Cs at individual horizons. ^{137}Cs horizons incorporate the first appearance in sediment columns (1952–1954), the fallout maximum (1963–1964) from atmospheric testing of nuclear bombs, the Chernobyl accident (1986), and the Fukushima Daiichi Nuclear Power Plant incident (2011).

Computation of wetland life

The seasonal wetland, ephemeral wetland, or intermittent wetland diminish seasonally; the wetlands were put forth to investigate the age of the wetland, and it is no longer useful for water activities. The diminishing activity of the wetland is due to the alarming sedimentation rate, and it cannot fulfill the water essential. The wetlands should be monitored, and suitable restoration and preservation controls should be planned (Singh et al. 2008). Wetland life was determined by considering the average sedimentation rate in conjunction with the ratio of the mean lake depth in its surroundings. The formulae adopted to determine the lifespan of Perumal lake are given as follows,

$$L_U = D_m \times \frac{100}{S_R} \quad (9)$$

where L_U is the useful life of the wetland (in years); D_m is the mean depth of the wetland (in m); S_R is the rate of sedimentation by ^{210}Pb and ^{137}Cs (in cm/year).

Result and discussion

Bulk density, porosity, and water content

The bulk density in the core sediment ranges from 1.04 to 2.19 g/cm^3 , averaging 1.52 g/cm^3 and the porosity of the sediments expresses from 2.76% to 53.97%, with a mean value of 32.47%, and followed by water content varies from 0.26% to 4.57%, with the average of 1.61% as shown in Fig. 2; Table 2. From the findings, the porosity and bulk density have been inversely proportional, indicating that the porosity increases eventually as the bulk density decreases (Fig. 2). In the sediment cores from Perumal Lake, it is notable that bulk density steadily increases with depth, attributed to the gradual compaction of overlying sediments, as observed in the study by Aja et al. (2015). Subsequently, the water content of the core sediments argues there is no significant relationship with the porosity of the core sediments.

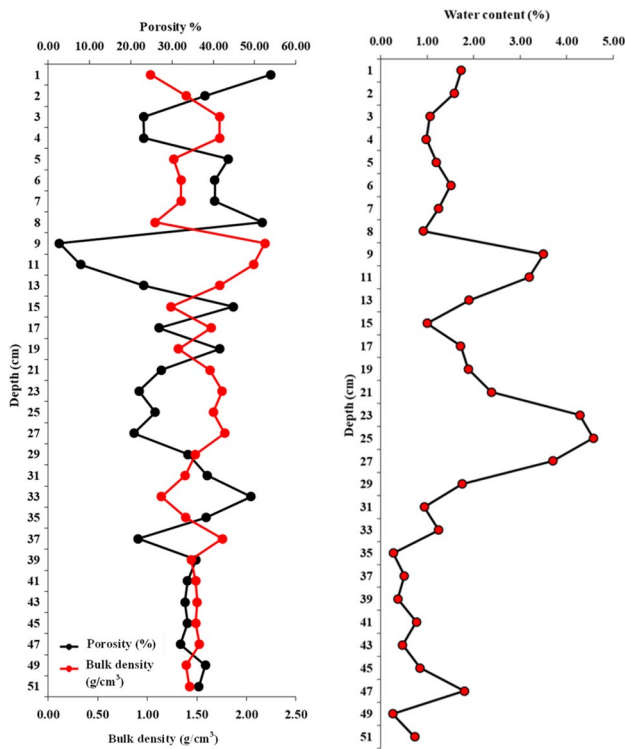


Fig. 2 Vertical profile of sand %, silt %, and clay % in the core sediments of the Perumal Lake

Analysis of the Characteristics of sediment deposition environments

The sediment textures in the Perumal wetland can be classified into three categories: sand (> 63 μm), silt (> 2 and < 63 μm), and clay (< 2 μm). The composition includes sand ranging from 0 to 5% with an average of 2%, silt varying from 0 to 8% with an average of 3%, and clay fluctuating from 87 to 100% with an average of 95% across the core profile. The pronounced predominance of clay content suggests a ‘low-energy environment’ (Table 3 and Fig. 3).

Analysis of the effect of grain size on ²¹⁰Pb_{exc} activity

The investigation on the effects of grain size in the ²¹⁰Pb_{exc} activities possessing the clay content attains more importance to absorption of the ²¹⁰Pb_{exc} in the sediments supplied from the atmospheric input and river or meltwater. Several researchers suggest clay is the main controlling factor for the ²¹⁰Pb_{exc} concentration in smaller particles with larger specific surface areas (He and Walling 1996). Sun et al. (2017) proposed that the ²¹⁰Pb activity of the clay is 24.7 times that of the sand and 3.2 times more that of the silt composition.

Table 2 Bulk density (g/cm³), water content (%), and porosity (%) in the core sediments of Perumal Lake

Depth in cm	Bulk density (g/cm ³)	Water content %	Porosity(%)
1	1.04	1.73	53.97
2	1.40	1.58	37.92
3	1.73	1.06	23.10
4	1.73	0.98	23.16
5	1.27	1.20	43.64
6	1.34	1.51	40.33
7	1.34	1.25	40.35
8	1.08	0.92	51.92
9	2.19	3.50	2.76
11	2.07	3.19	7.85
13	1.73	1.90	23.16
15	1.24	1.00	44.84
17	1.65	1.72	26.86
19	1.31	1.88	41.56
21	1.63	2.38	27.38
23	1.76	4.28	22.00
25	1.67	4.57	25.91
27	1.78	3.70	20.82
29	1.49	1.75	33.88
31	1.38	0.94	38.53
33	1.14	1.25	49.17
35	1.39	0.27	38.23
37	1.76	0.51	21.81
39	1.44	0.37	35.80
41	1.49	0.77	33.79
43	1.50	0.47	33.15
45	1.49	0.85	33.78
47	1.53	1.80	32.08
49	1.39	0.26	38.11
51	1.43	0.73	36.52
Min	1.04	0.26	2.76
Max	2.19	4.57	53.97
Avg	1.52	1.61	32.47

Correlation analysis of the sediment composition shows the relationship between depth and ²¹⁰Pb_{exc} activities. The strong positive relationship of core sediments between the finer fraction (Clay) and depth unveils the higher content of ²¹⁰Pb in the vertical core profile.

Analysis of the vertical profiling of ²¹⁰Pb

According to the CRS model, the ²¹⁰Pb_{exc} dating is significantly assigned to conduct the sediment age and accumulation rates (Sanchez-Cabeza et al. 1999). Measurements of ²¹⁰Pb radionuclide, the core sediment were sliced into 1 cm intervals, and the intermittent samples were undergone

Table 3 Percentage of sand, silt, and clay in the core sediments of Perumal Lake

Depth	Sand	Silt	Clay
1	1.2	2.8	96
2	2.6	3.4	94
3	2.1	2.9	95
4	2.1	1.9	96
5	1.8	4.2	94
6	2.2	4.8	93
7	1.7	6.3	92
8	3.5	5.5	91
9	3	7	90
11	5	8	87
13	4	7	89
15	4	5	91
17	4	6	90
19	2.1	2.9	95
21	4	2	94
23	3.2	4.8	92
25	0	0	100
27	3	7	90
29	1.5	2.5	96
31	2	5	93
33	1.4	1.6	97
35	0	2	98
37	0	0	100
39	0	0	100
41	0	2	98
43	0	0	100
45	0.2	0.8	99
47	0	1	99
49	0	0	100
51	0	0	100
Min	0	0	87
Max	5	8	100
Avg	2	3	95

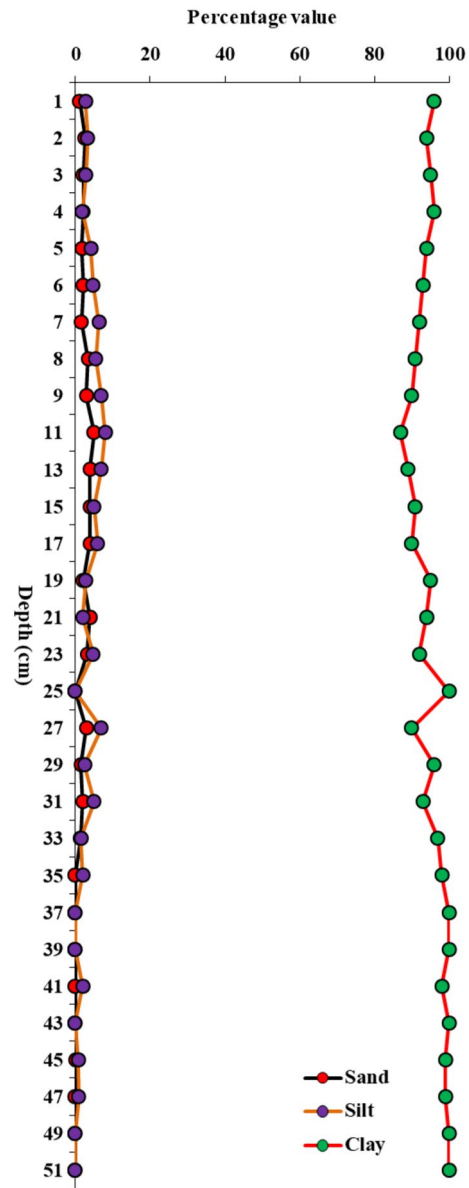


Fig. 3 Vertical profile of Bulk density (in g/cc), water content (in %), and porosity (in %) in the core sediments of the Perumal Lake

for analysis. The value of $^{210}\text{Pb}_{\text{exc}}$ ranges from 5.44 ± 0.43 (Bq/kg) to 80.12 ± 6.40 (Bq/kg), with a mean value of 27.27 ± 2.09 (Bq/kg), as shown in Table 4. The oldest layer of the vertical core profile at a depth of 51 cm represents the age of 1944 AD. The mean accumulation rate ($\text{kg/m}^2/\text{year}$) and sedimentation rate (cm/year) of core sediments implies 0.57 ± 0.05 ($\text{kg/m}^2/\text{year}$) and 0.84 ± 0.07 (cm/year) dated from 1944 to 2023 AD, and to discuss the increase and decreasing criteria in the sediment deposits within the wetland supervened by various reasons.

Notably, the accumulation rate of core sediments has increased towards the top layers compared to the bottom layers. Additionally, the $^{210}\text{Pb}_{\text{exc}}$ sedimentation rate demonstrates peak values beneath the top layers, indicating that the uppermost layer experiences disturbance primarily from river inputs, as highlighted in the study by Hancock

and Hunter (1999). Conspicuously, the core sediment findings imply the maximum sedimentation rate has been noted as 1.37 ± 0.11 (cm/year), and the rate of accumulation is 2.38 ± 0.19 ($\text{kg/m}^2/\text{year}$) at a depth of 2 cm dated since 2022AD. Furthermore, another maximum sedimentation rate of 1.36 ± 0.11 (cm/year) accumulation rate is 5.29 ± 0.42 ($\text{kg/m}^2/\text{year}$) at a depth of 1 cm dated as 2023AD. From 1944 to 1992AD, the sedimentation rate gradually increased at the depth of 51 cm to 33 cm, with a mean value of 0.62 ± 0.05 (cm/year), as shown in Fig. 4.

Additionally, the sedimentation rate fluctuation in the core sediments may be due to the nuclear tests in 1970AD, considered as the key marker for the auxiliary value of ^{137}Cs

Table 4 Age dating and sedimentation rate based on the CRS method of ^{210}Pb radionuclide in the core sediments of Perumal Lake

Depth	$^{210}\text{Pb}_{\text{exc}}$ (Bq/kg)	Mass flux(kg/m ²)	Inventory $^{210}\text{Pb}_{\text{exc}}$ (Bq/m ²)	Cumulative $^{210}\text{Pb}_{\text{exc}}$ (Bq/m ²)	Estimated Year	Date	Accumulation rate (kg/m ² /y)	Sedimentation rate (cm/y)
1	21.79 ± 1.74	3.88	84.49	3759.23	0.73	2023	5.29 ± 0.42	1.36 ± 0.11
2	23.45 ± 1.87	3.48	81.57	3674.74	1.46	2022	2.38 ± 0.19	1.37 ± 0.11
3	24.32 ± 1.94	4.05	98.54	3593.17	2.35	2021	1.72 ± 0.14	1.27 ± 0.10
4	25.15 ± 2.01	3.79	95.40	3494.62	3.25	2020	1.17 ± 0.09	1.23 ± 0.10
5	30.25 ± 2.42	4.44	134.27	3399.22	4.55	2019	0.98 ± 0.08	1.10 ± 0.09
6	39.15 ± 3.13	3.31	129.51	3264.95	5.85	2018	0.57 ± 0.05	1.02 ± 0.08
7	38.12 ± 3.04	4.28	163.26	3135.44	7.58	2016	0.57 ± 0.05	0.92 ± 0.07
8	21.05 ± 1.68	7.01	147.49	2972.19	9.22	2017	0.76 ± 0.06	0.87 ± 0.07
9	41.57 ± 3.32	4.41	183.24	2824.70	11.38	2015	0.39 ± 0.03	0.79 ± 0.06
11	56.13 ± 4.49	6.19	347.56	2641.46	15.93	2011	0.39 ± 0.03	0.69 ± 0.06
13	24.32 ± 1.94	3.34	81.26	2293.90	17.10	2009	0.2 ± 0.02	0.76 ± 0.06
15	32.19 ± 2.57	5.36	172.67	2212.64	19.72	2007	0.27 ± 0.02	0.76 ± 0.06
17	53.51 ± 4.28	4.53	242.15	2039.97	23.79	2003	0.19 ± 0.02	0.71 ± 0.06
19	24.32 ± 1.94	3.48	84.60	1797.82	25.35	2002	0.14 ± 0.01	0.75 ± 0.06
21	7.22 ± 0.57	4.05	29.26	1713.22	25.91	2002	0.16 ± 0.01	0.81 ± 0.06
23	20.17 ± 1.61	7.01	141.32	1683.96	28.73	1999	0.24 ± 0.02	0.80 ± 0.06
25	15.05 ± 1.20	4.41	66.34	1542.64	30.15	1997	0.15 ± 0.01	0.83 ± 0.07
27	12.58 ± 1.00	6.19	77.90	1476.30	31.90	1996	0.19 ± 0.02	0.85 ± 0.07
29	22.57 ± 1.80	3.48	78.51	1398.40	33.76	1994	0.10 ± 0.01	0.86 ± 0.07
31	5.44 ± 0.43	4.44	24.15	1319.89	34.36	1993	0.13 ± 0.01	0.90 ± 0.07
33	7.76 ± 0.62	3.31	25.67	1295.74	35.00	1992	0.09 ± 0.01	0.94 ± 0.08
35	80.12 ± 6.40	4.53	362.57	1270.07	45.85	1986	0.1 ± 0.01	0.76 ± 0.06
37	26.7 ± 2.13	5.39	144.00	907.50	51.42	1978	0.1 ± 0.01	0.72 ± 0.06
39	17.17 ± 1.37	4.05	69.57	763.50	54.50	1976	0.07 ± 0.01	0.72 ± 0.06
41	29.31 ± 2.34	7.01	205.37	693.93	65.82	1971	0.11 ± 0.01	0.62 ± 0.05
43	33.24 ± 2.65	4.41	146.52	488.56	77.32	1957	0.06 ± 0.005	0.56 ± 0.04
45	23.92 ± 1.91	7.01	167.60	342.04	99.04	1950	0.07 ± 0.01	0.45 ± 0.04
47	12.72 ± 1.01	4.41	56.07	174.44	111.55	1945	0.04 ± 0.003	0.42 ± 0.03
49	9.65 ± 0.77	6.19	59.75	118.37	134.22	1944	0.05 ± 0.004	0.37 ± 0.03
51	8.11 ± 0.65	7.23	58.62	58.62				
Min	5.44 ± 0.43							
Max	80.12 ± 6.40							
Avg	27.27 ± 2.09						0.57 ± 0.05	0.84 ± 0.07

in the atmospheric depositions, and the industrial revolution 1960s and Chernobyl accident in 1986AD tends to increase the heat radiation in the atmosphere throughout the world unveils the rapid retreat the glaciers to increases the sediment transportation and deposition in the high altitude wetlands (Das and Vasudevan 2021; Rout and Vasudevan 2022).

Many researchers have investigated the sediment accumulation rate in the different parts of the Himalayan and Eastern Ghats wetland regions to compare it with that of Perumal Lake. The increased sediment accumulation rate in recent years can be attributed to silicate weathering and carbonate weathering, as well as anthropogenic influences from mining activities, tourism, residents, and ongoing

construction activities. The sediment accumulation rate of the other wetlands, such as Bhimtal (0.22 kg/m²/year; Das et al. 1994), Nainital (0.86 kg/m²/year), Naukuchiatal (0.42 kg/m²/year), Sattal (0.3 kg/m²/year) (Kumar et al. 1999c), Mansar (0.89 kg/m²/year; Rai et al. 2007a), Satopanth (0.31 kg/m²/year; Das and Vasudevan 2021), Pykara (0.26 kg/m²/year; Singh and Vasudevan 2021), Chandratat (0.63 kg/m²/year; Rout and Vasudevan 2022), and Kodai-kanal (1.00 kg/m²/year; Palani et al. 2023). The Nainital wetland in the Himalayan region shows an accumulation rate due to anthropogenic activities. On the other hand, the wetlands were dominated by the weathering of carbonate rocks in the regions (Rai et al. 2007a). The accumulation

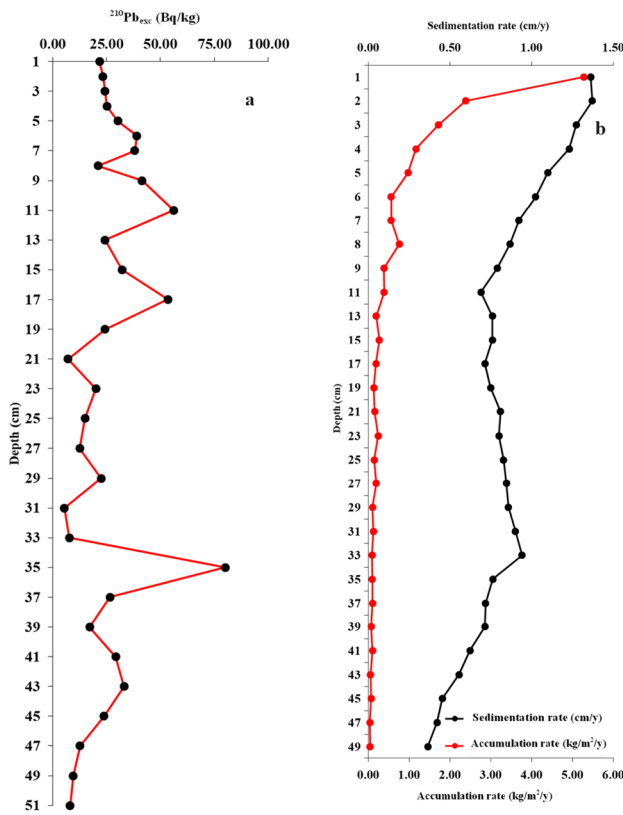


Fig. 4 $^{210}\text{Pb}_{\text{exc}}$ activity shows in the temporal profile (a) and sedimentation rate (cm/y) and Accumulation rate ($\text{kg}/\text{m}^2/\text{y}$) shows in (b) of the core sediments

rate of Mansar wetland possesses more sediments due to the fine-grained sandstones alternating with siltstone, mudstone, and clay eroded by the Siwalik region of the lesser Himalayas. The elevated activity of ^{210}Pb in the sediments can be accounted as atmospheric fallouts to rivers and lakes; heavy precipitation plays a vital role in transporting the fine particles to the lake environs and, followed by the radionuclide trapped in the mud contents because of deforestation, agricultural works, industrial activities and tourism in the Kodaikanal Lake. The sedimentation rate of some other wetlands examined by the researchers noted that the variation in the sedimentation rate does not depend on similar climatic conditions in the areas. To save the wetland, the necessary action must be taken to avoid the enormous sedimentation rate in the wetlands (Sarkar et al. 2016).

Analysis of vertical profiling of ^{137}Cs dating

Despite knowing that ^{137}Cs is a marker of sedimentation processes that tightly bind predominantly to the clay lattice, including silt, with a long half-life (30.2 ± 0.1 years) (Francis and Brinkley 1976), it can also be considered to be

Table 5 Age dating and mean sedimentation rate of ^{137}Cs radionuclide in the core sediments of Perumal Lake

Depth (cm)	^{137}Cs (Bq/kg)	Date (y)	Estimated year (y)	Mean Sedimentation rate (cm/y) – 1963& 1986
1	14 ± 0.88	2021	2	
2	18 ± 1.13	2019	4	
3	13 ± 0.82	2018	5	
6	9.0 ± 0.57	2012	11	0.57 ± 0.04
7	33 ± 2.08	2011	12	
9	18.3 ± 1.15	2007	16	0.43 ± 0.03
10	17 ± 1.07	2005	18	
11	9.4 ± 0.59	2004	19	
14	10.7 ± 0.67	1998	25	
16	27.4 ± 1.73	1995	28	
20	11.2 ± 0.71	1988	35	
21	19.1 ± 1.20	1986	37	
23	10.2 ± 0.64	1982	41	
25	16.4 ± 1.03	1979	44	
26	21.1 ± 1.33	1977	46	
28	24.2 ± 1.52	1974	49	
29	3.1 ± 0.20	1972	51	
30	2.0 ± 0.13	1970	53	
31	2.6 ± 0.16	1968	55	
33	11.9 ± 0.75	1965	58	
34	44.6 ± 2.81	1963	60	
35	2.5 ± 0.61	1961	62	
37	1.4 ± 0.09	1958	65	
39	1.6 ± 0.10	1954	69	
41	2.5 ± 0.16	1951	72	
43	1.9 ± 0.12	1947	76	
45	1.5 ± 0.10	1944	79	
47	1.6 ± 0.10	1940	83	
49	1.1 ± 0.07	1937	86	
Min	1.1 ± 0.07			
Max	44.6 ± 2.81			
Avg	12.78 ± 0.81			

exchangeable by the sediment (Smith and Comans 1996). There are two approaches to examining the ^{137}Cs : the horizon and peak methods. The sedimentation rate of the ^{137}Cs method was augmented by adopting 1963 as the key marker to construct the age profile for Perumal Lake (1937AD to 2021AD), as shown in Table 5.

In the study area, the core sediment concerning the ^{137}Cs was used to examine the sedimentation rate and age of the core profile in the wetland. The value of ^{137}Cs ranges from 1.1 ± 0.07 (Bq/kg) to 44.6 ± 2.81 (Bq/kg), with a mean value of 12.78 ± 0.81 (Bq/kg), as shown in Table 5. The most significant spikes of ^{137}Cs in the core profile possessing at 1963AD and 2011AD at a depth of 34 cm and 7 cm indicate the nuclear test year of 1963AD inferred as 44.6 ± 2.81 (Bq/

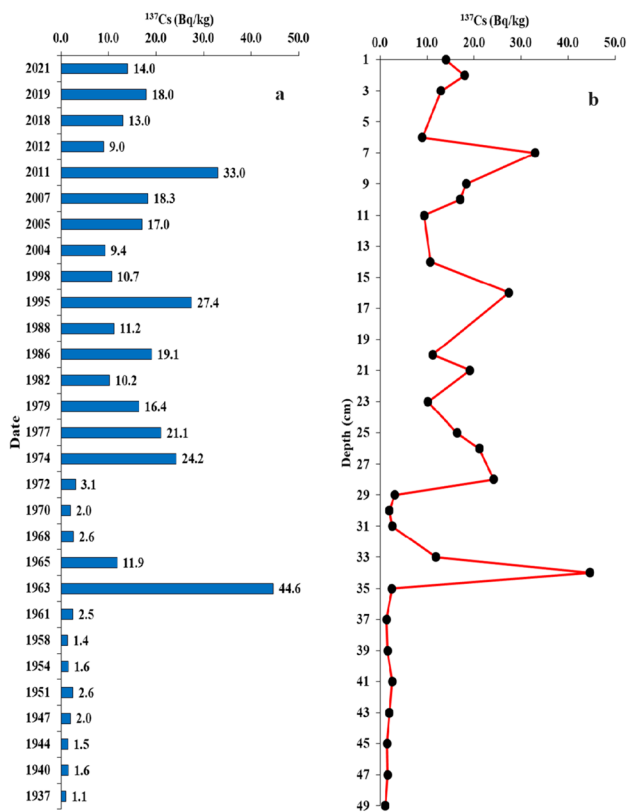


Fig. 5 Temporal profile of ¹³⁷Cs (Bq/kg) activity represented in **a** age and **b** depth profile in the core sediments of the Perumal Lake

kg), and the Fukushima Daiichi 2011 indicates 33 ± 2.08 (Bq/kg). The ¹³⁷Cs activity remained relatively stable below 1963, reflecting minimal cesium input in the sediments. However, a notable secondary peak of 24.2 ± 1.52 (Bq/kg) at 28th cm depth emerged post-1963, representing the peak fallout from nuclear bomb testing. Furthermore, another peak at 16th cm depth displaying 27.4 ± 1.73 (Bq/kg) indicates increased ¹³⁷Cs activity post the Chornobyl incident 1986, as depicted in Fig. 5. Various studies have investigated the ¹³⁷Cs activity in core sediments, revealing different ranges such as in Kodaikanal Lake 3.5 ± 0.1 to 22.04 ± 1.4 Bq/kg (Palani et al. 2023), Satopanth Tal 2.48 ± 0.1 to 7.24 ± 0.1 Bq/kg (Das and Vasudevan 2021), Chandratat 2 ± 0.2 to 165 ± 0.3 Bq/kg (Rout and Vasudevan 2022), and Pykara Lake 1.21 ± 0.1 to 17.15 ± 1.7 Bq/kg (Singh and Vasudevan 2021).

The Mean sedimentation rate of the core for pivotal marker years 1963 and 1986 represents 0.57 ± 0.04 (cm/year) and 0.43 ± 0.03 (cm/year), respectively. This should happen because of a year difference between the marker times or instrumentation ambiguity. Regional aspects such as human activity, regional catchment/limnological processes, and

sediment mixing may be accountable for this phenomenon. The overall age of the ¹³⁷Cs core sediment from Perumal Lake has been calculated to be 86 years.

Analysis of the life of the wetlands

To decode the life computation, the Perumal Lake accounted for the sedimentation rate in the single zone, volume of the wetland, and mean depth (Singh et al. 2008). From the valuable findings, the Lake lifespan is around 369.05 years and 543.86 years concerning ²¹⁰Pb and ¹³⁷Cs, respectively. In this context, radionuclide dating, such as ²¹⁰Pb and ¹³⁷Cs, is considered to identify the sedimentation rate and the recent age module to assess the life of the lake.

Conclusion

The comprehensive analysis conducted in March 2023 on core sediments from Perumal Lake, Cuddalore district, Tamil Nadu, utilizing ²¹⁰Pb and ¹³⁷Cs radionuclide activity, has provided valuable insights into the sedimentation patterns and age profiles. Several significant findings have emerged from our meticulous investigation. The bathymetric study has revealed key morphometric characteristics, establishing the lake's dimensions at 11.54 km in length with an average depth of 3.1 m. The temporal relationship between bulk density and porosity suggests an inverse correlation, indicating the sediment's behavior. Granulometric analysis has revealed a predominance of a low-energy environment within the lake, characterized by a 100% clay composition. The association between clay content and ²¹⁰Pb activity underscores the efficient trapping of ²¹⁰Pb in the core sediments. Furthermore, the accumulation rate is notably higher in the upper sections of the core sediments compared to the lower sections. The heightened ²¹⁰Pb activity in the sediments is attributed to atmospheric fallout transported by heavy precipitation, exacerbated by deforestation, local human activities, mining, agriculture, and industry. Our study underscores the critical influence of dynamic sediment accumulation rates on the wetland's longevity.

The calculated sedimentation rates using ²¹⁰Pb and ¹³⁷Cs radionuclides indicate an estimated lifespan of 369.05 years and 543.86 years, respectively. This suggests relative stability in the current environmental conditions. However, proactive measures are imperative to address and regulate the elevated sedimentation rates in Perumal Lake and safeguard the wetland ecosystem from rapid degradation. Future research endeavors should consider employing numerical simulations to delve deeper into the responses of different wetland areas to ²¹⁰Pb and ¹³⁷Cs activities, offering more profound insights for effective wetland management strategies.

Acknowledgements The authors acknowledge the support of Annamalai University, Tamil Nadu, India, for providing necessary laboratory facilities for the sample analysis. The authors are also immensely thankful to R.K. Singhal, Head, his research team, Analytical Spectroscopy Section, Department of Analytical Chemistry Division, Bhabha Atomic Research Centre (BARC), Mumbai, India, for requisite support at different stages of this work.

Author contributions Sivaprakasam Vasudevan oversaw data collection and original manuscript as well as did the supervision, Baranidharan Sathyanarayanan produced the modeling, interpretation and original manuscript draft. Vijayakumar V contributes to writing, interpretation. Sivaranjan Periyasami and Pravinraj Sambath contribute to review the original draft for the enrichments.

Data availability No datasets were generated or analysed during the current study.

Code availability Not applicable.

Declarations

Competing interests The authors declare no competing interests.

Ethics approval Not applicable.

Consent to participate Not applicable.

Consent for publication Not applicable.

References

- Aja K, Dr R, Karpe R, Mishra M, Narayanan U, Singhal R, Ravi P, Tripathi R (2015) Inventory, fluxes, and residence times from the depth profiles of naturally occurring ^{210}Pb in marine sediments of Mumbai Harbor Bay. *Environ Earth Sci* 73(8):4019–4031. <https://doi.org/10.1007/s12665-014-3687-6>
- Albrecht A, Reiser R, Luck A, Stoll JM, Giger W (1998) Radiocesium dating of sediments from wetlands and reservoirs. *Environ Sci Technol* 32(13):1882–1887
- Alhajji E, Ismail IM, Al-Masri MS, Salman N, Al-Haleem MA, Doubal AW (2014) Sedimentation rates in the Lake Qattinah using ^{210}Pb and ^{137}Cs as geochronometer. *Geochronometria* 41:81–86. 10.2478/s13386-013-0142-5
- Al-Masri MS, Mamish S, Budier Y (2003) Radionuclides and trace metals in eastern Mediterranean Sea algae. *J Environ Radioact* 65(2):157–168
- Appleby PG (2001) Chronostratigraphic techniques in recent sediments. Tracking environmental change using lake sediments: basin analysis, coring, and chronological techniques, Kluwer Academic Publishers, Dordrecht 171–203
- Appleby PG, Oldfield F (1978) The calculation of lead-210 dates assuming a constant rate of supply of unsupported ^{210}Pb to the sediment. *CATENA* 5(1):1–8. [https://doi.org/10.1016/S0341-8162\(78\)80002-2](https://doi.org/10.1016/S0341-8162(78)80002-2)
- Appleby PG, Oldfield F (1992) Applications of lead-210 to sedimentation studies. In *Uranium-series disequilibrium: applications to earth, marine, and environmental sciences 2*
- Bedient PB, Huber WC (1992) *Hydrology and Flood Plain Analysis*, 2nd edn. Addison-Wesley, New York
- Bhat SA, Pandit AK (2014) Surface water quality assessment of Wular-lake, ARamsar Site in Kashmir, Himalaya, using discriminate analysis and WQI. *J Ecosyst* 1–18
- Burrough PA, McDonnell RA (1998) *Principles of geographical information systems*. Oxford University Press, Oxford
- Butler D (2011) Radioactivity spreads in Japan: fallout is localized, but could persist for years in some regions. *Nature* 471(7340):555–556
- Chandrakiran KS (2013) Assessment of physicochemical characteristics of sediments of a lower Himalayan Wetland, Mansar, India. *Int Res J Environ Sci* 2(9):16–22
- Cheng Z, Wang XH, Jalon-Rojas I, Liu Y (2019) Reconstruction of sedimentation changes under anthropogenic influence in a medium-scale estuary based on a decadal chronological framework. *Estuar Coast Shelf Sci* 227:106295. <https://doi.org/10.1016/j.ecss.2019.106295>
- Chino M, Nakayama H, Nagai H, Terada H, Katata G, Yamazawa H (2011) Preliminary estimation of release amounts of ^{131}I and ^{137}Cs accidentally discharged from the Fukushima Daiichi nuclear power plant into the atmosphere. *J Nucl Sci Technol (Tokyo)* 48(7):1129–1134
- Corcoran M, Sherif MI, Smalley C, Li A, Rockne KJ, Giesy JP, Sturchio NC (2018) Accumulation rates, focusing factors, and chronologies from depth profiles of ^{210}Pb and ^{137}Cs in sediments of the Laurentian Great Lakes. *J Great Lakes Res* 44(4):693–704. <https://doi.org/10.1016/j.jglr.2018.05.013>
- Das S, Vasudevan S (2021) A comprehensive study on sedimentation rate and sediment age of Satopanth Tal Garhwal Himalaya, using ^{210}Pb and ^{137}Cs techniques. *J Radioanal Nucl Chem* 329(2):633–646
- Das BK, Singh M, Borkar MD (1994) Sediment accumulation rate in the lakes of Kumaun Himalaya, India using ^{210}Pb and ^{226}Ra . *Environ Geol* 23(2):114–118
- Diwate P, Meena N, Bhushan R, Pandita S, Chandana KR, Kumar P (2020) Sedimentation rate (^{210}Pb and ^{137}Cs), grain size, organic matter, and bathymetric studies in Renuka Lake, Himachal Pradesh India. *Himal Geol* 41:51–62
- Edgington DN, Klump JV, Robbins JA, Kusner YS, Pambura VD, Santimirov IV (1991) Sedimentation rates residence time and radionuclide inventories in Lake Baikal from ^{137}Cs and ^{210}Pb in sediment cores. *Nature* 350:601–604
- Fairbridge RW (1968) *Glacier Wetlands*. In: Fairbridge RW (Ed.), *The encyclopedia of geomorphology*, Reinhold 444–453
- Francis C, Brinkley F (1976) Preferential adsorption of ^{137}Cs to micaceous minerals in contaminated freshwater sediment. *Nature* 260:511–513. <https://doi.org/10.1038/260511a0>
- Gharibreza M, Raj JK, Yusof I (2013) Sedimentation rates in Bera Lake (Peninsular Malaysia) using ^{210}Pb and ^{137}Cs radioisotopes. *Geosci J* 17:211–220. <https://doi.org/10.1007/s12303-013-0013-3>
- Goldberg ED (1963) *Geochronology with lead-210, radioactive dating*, IAEA. Vienna 1:21–131
- Guan YJ, Chen W, Wang SZ, Hua YX, Jing QY, Liu ZY, Guo ZC (2023) First application of plutonium in soil erosion research on terraces. *Nucl Sci Tech* 34(4):51
- Guan Y, Cui L, Huang C, Guo Z, Fan K, Wang H, Liu Z (2024) Migration of fallout radionuclides and soil erosion of hongsongwa mountainous in China. *ACS Earth Space Chem* 8(5):1000–1010
- Guo J, Costa OS, Wang Y, Lin W, Wang S, Zhang B, Zhang L (2020) Accumulation rates and chronologies from depth profiles of ^{210}Pb and ^{137}Cs in sediments of northern Beibu Gulf, South China sea. *J Environ Radioact* 213:106136. <https://doi.org/10.1016/j.jenvrad.2019.106136>
- Hancock GJ, Hunter JR (1999) Use of excess ^{210}Pb and ^{228}Th to estimate rates of sediment accumulation and bioturbation in Port Phillip Bay, Australia. *Mar Freshw Res* 50:533–545. <https://doi.org/10.1071/MF98053>
- He Q, Walling DE (1996) Interpreting particle size effects in the adsorption of ^{137}Cs and unsupported ^{210}Pb by mineral soils and sediments. *J Environ Radioact* 30(2):117–137

- Henderson GM, Lindsay FN, Slowey NC (1999) Variation in bioturbation with water depth on the marine slope: A study on the Little Bahamas Bank. *Mar Geol* 160:105–118
- Humane SS, Humane SK, Juare S (2016) Pb dating and trace metal 210 accumulation study of sediment cores from NavegaonBandh and Bodhalkasa Lakes, Gondia District, Maharashtra India. *Environ Earth Sci* 75(7):602. <https://doi.org/10.1007/s12665-016-5371-5>
- Khadka UR, Ramanathan AL (2013) Major ion composition and seasonal variation in the lesser Himalayan Lake: case of Begnas Lake of the Pokhara valley, Nepal. *Arab J Geosci* 4191–4206
- Kothari UC (1996) Erosion and sedimentation problems in India. *IAHS PublSerProc Rep Intern AssocHydroSci* 236:531
- Krishnaswamy S, Lal D, Martin JM, Meybeck M (1971) Geochronology of lake sediments. *Earth Planet SciLett* 11(1–5):407–414
- Kumar B, Rmp N, Rai SP, Kumar US, Navada SV (1999a) Improved prediction of life of a Himalayan Wetland. *Mt Res Dev* 19:113–121
- Kumar B, Jain SK, Nachiappan RMP, Rai SP, Kumar V, Dungrakoto VC; Rawat YS (1999b) Hydrological studies of Wetland Nainital, Kumaun Himalayas, Uttar Pradesh. Project Report, National Institute of Hydrology, Roorkee, India 21
- Kumar U, Navada S, Rao S, Nachiappan RM, Kumar B, Krishnamoorthy T, Jha S, Shukla V (1999c) Determination of recent sedimentation rates and patterns in Wetland Naini, India by 210Pb and 137Cs dating techniques. *Appl Radiat Isotopes* 51:97–105. [https://doi.org/10.1016/S0969-2058043\(98\)00148-1](https://doi.org/10.1016/S0969-2058043(98)00148-1)
- Kumar B, Rai S, Nachiappan RP, Kumar US, Singh S, Diwedi VK (2007) Sedimentation rate in North Indian lakes estimated using 137Cs and 210Pb dating techniques. *Curr Sci* (00113891): 92(10)
- Kumar A, Singhal RK, Preetha J, Rupali K, Narayanan U, Suresh S, Mishra MK, Ranade AK (2008) Impact of a tropical ecosystem on the migrational behaviour of K-40, Cs-137, Th-232 U-238 in perennial plants. *Water Air Soil Pollut* 192:293–302
- Kusumgar S, Agrawal DP, Sharma P (1989) Radiocarbon chronology and magnetic susceptibility variation in Kumaon Wetland sediments. *Radiocarbon* 31:957–964
- Liang Kangkang Hu, Xinxin LS, Chengmin H, Ya T (2014) Anthropogenic effect on deposition dynamics of Wetland sediments based on 137Cs and 210Pbex techniques in Jiuzhaigou National Nature Reserve. *China Chinese Geograph Sci* 24(2):180–190. <https://doi.org/10.1007/s11769-014-0665-6>
- Mondal D, Pal J, Ghosh TK, Biswas AK (2012) Abiotic characteristics of Mirik lake water in the hills of Darjeeling, West Bengal, India. *Adv Appl Sci Res J* 3(3):1335–1345
- Nautiyal H, Bhandari SP, Sharma RC (2012) Physico-chemical study of Dodital Lake in Uttarkashi District of Garhwal Himalaya. *Int J Sci Technol Res* 1(5):58–60
- Palani B, Vasudevan S, Ramkumar T, Rajendiran S (2021) An investigation on the assessment of mercury concentration and its spatial distribution in Kodaikanal Lake sediments, South India. *Arab J Geosci* 14:1–12
- Palani B, Vasudevan S, Ramkumar T, Rajendiran S, Gunasekaran S (2023) Determination of sedimentation rates and life of Kodaikanal Lake, South India, using radiometric dating (210Pb and 137Cs) techniques. *Environ Earth Sci* 82(9):228
- Putyrskaya V, KlemE RS, Corcho-Alvarado JA, Sahli H (2020) Dating of recent sediments from Lago Maggiore and Lago di Lugano (Switzerland/Italy) using 137Cs and 210Pb. *J Environ Radioact* 212:106135
- Rai SP, Kumar V, Kumar B (2007a) Sedimentation rate and pattern of a Himalayan foothill lake using 137Cs and 210Pb. *Hydro Sci J* 52(1):181–191
- Rai SP, Kumar V, Kumar B (2007b) Sedimentation rate and pattern of a Himalayan foothill wetland using 137Cs and 210Pb. *Hydro Sci J* 52(1):181–191. <https://doi.org/10.1623/hysj.52.1.181>
- Ritchie JC, McHenry JR (1990) Application of radioactive fallout cesium-137 for measuring soil erosion and sediment accumulation rates and patterns: a review. *J Environ Qual* 19:215. <https://doi.org/10.2134/jeq1990.00472425001900020006x>
- Robbins JA, Edgington DN, Kemp AL (1978) Comparative 210Pb, 137Cs, and pollen geochronologies of sediments from Lakes Ontario and Erie. *Quat Res* 10(2):256–278
- Rout SP, Vasudevan S (2022) Sedimentation rates and sediment age of the high-altitude cold desert Ramsar Wetland, the Chandratlal, inferred from radionuclide (²¹⁰Pb and ¹³⁷Cs) technique. *Environ Monit Assess* 194(4):305–540
- San Miguel EG, Bolivar JP, Garcia-Tenorio R (2004) Vertical distribution of Th-isotope ratios, 210Pb, 226Ra, and 137Cs in sediment cores from an estuary affected by anthropogenic releases. *Sc Tot Environ* 318:143–157
- Sanchez-Cabeza JA, Masque P, Ani-Ragolta I (1998) 210Pb and 210Po analysis in sediments and soils by microwave acid digestion. *J Radioanal Nucl Chem* 227:19–22
- Sanchez-Cabeza JA, Masque P, Ani-Ragolta I, Merino J, Frignani M, Alvisi F, Palanques AP, Puig P (1999) Sediment accumulation rates in the southern Barcelona continental margin (NW Mediterranean Sea) derived from 210Pb and 137Cs chronology. *Prog Oceanogr* 44:313–332
- Sarkar S, Prakasam M, Banerji US, Bhushan R, Gaury PK, Meena NK (2016) Rapid sedimentation history of Rewalsar Lake, Lesser Himalaya, India during the last fifty years—Estimated using Cs-137 and Pb-210 dating techniques: a comparative study with other North-Western Himalayan Lakes. *Himalayan Geol* 37(1):1–7
- Semertizidou P, Piliposian GT, Chiverrell RC (2019) Long-term stability of records of fallout radionuclides in the sediments of Brotherswater, Cumbria (UK). *J Paleolimnol* 61:231–249. <https://doi.org/10.1007/s10933-018-0055-7>
- Sert I, Ozel FE, Yaprak G, Eftelioglu M (2016) Determination of the latest sediment accumulation rates and pattern by performing 210 Pb models and 137 Cs technique in the Lake Bafa, Mugla, Turkey. *J Radioanal Nucl Chem* 307:313–323
- Shah C, Banerji US, Chandana KR, Bhushan R (2020) 210Pb dating of recent sediments from the continental shelf of western India: factors influencing sedimentation rates. *Environ Monit Assess* 192(7):468. <https://doi.org/10.1007/s10661-020-08415-x>
- Singh KK, Vasudevan S (2021) Reconstruction of sedimentation rates based on the chronological framework of Lake Pykara, Tamil Nadu, India. *Environ Monitor Assess* 193(7):428
- Singh KS, Kumar B, Khare D, Jain SK (2007) Estimation of erosion rate in a small catchment of Loktak wetland, India, using lead-210 (210Pb) technique. *Int J Water* 3(3):257–265
- Singh S, Thakural LN, Kumar B (2008) Estimation of sediment rates and life of Sagar Lake using radiometric dating techniques. *Water Resour Manage* 22(4):443–455
- Singhal RK, Venkatesh M, Wagh DN, Basu H, Chavan T, Pimple MV, Reddy AVR (2012) Determination of chronological heavy metal deposition and pollution intensity in the bottom sediments of Mumbai Harbour Bay, India using 137Cs as a tracer. *J Radioanal Nucl Chem* 292(2):863–869
- Smith JT, Comans RNJ (1996) Modelling the difusive transport and remobilisation of 137Cs in sediments: the effects of sorption kinetics and reversibility *Geochim. Cosmochim Acta* 60:995–1004. [https://doi.org/10.1016/0016-7037\(96\)00030-0](https://doi.org/10.1016/0016-7037(96)00030-0)
- Strakhovenko V, Subetto D, Ovdina E, DanilenkoI BelkinaN, Efrementenko N, Maslov A (2020) Mineralogical and geochemical composition of Late Holocene bottom sediments of Lake Onego. *J Great Lakes Res* 46(3):443–455
- Sun X, Fan D, Tian Y, Shiwen Z (2017) Normalization of excess 210 Pb with grain size in the sediment cores from the Yangtze River Estuary and adjacent areas: implications for sedimentary

- processes. *The Holocene* 28(4): 545–557. <https://doi.org/10.1177/0959683617735591>
- Szarlowicz K, Reczynski W, Czajka A, Spyt B, Szacilowski G (2017) Comprehensive study of the mountainous lake sediments in relation to natural and anthropogenic processes and time (Mały Staw Lake, Poland). *Environ Sci Pollut Res* 25(4):3335–3347
- UNSCEAR (2000) Sources and effects of ionizing radiation, Report to the General Assembly, with Scientific Annexes, vol I. United Nations, New York
- Wentworth CK (1922) A scale of grade and class terms for clastic sediments. *J Geol* 5:377–392
- Wood AKH, Ahmad Z, Shazili NAM, Yaakob R, Carpenter R (1997) Geochemistry of sediments in Johore Strait between Malaysia and Singapore. *Continent Shelf Res* 17(10):1207–1228
- WWF (2005) An overview of glacial retreat and subsequent impacts in Nepal, India, and China. World Wide Fund for Nature, Nepal 1–79
- Zaborska A, Carroll J, Papucci C, Pempkowiak J (2007) Intercomparison of alpha and gamma spectrometry techniques used in ^{210}Pb geochronology. *J Environ Radioact* 93:38–50
- Zapata F (2002) Handbook for the assessment of soil erosion and sedimentation using environmental radionuclides Dordrecht: Kluwer Academic Publishers 219:9348054–9
- Zhang XB, Long Y, He XB, Wen AB, Yan DC (2012) Use of ^{137}Cs and ^{210}Pb peaks produced by events in the catchment for dating sediments in the Jiulongdian Reservoir, Chuxiong, Yunnan Province China. *IAHS356*: 378–384

Publisher's Note Springer Nature remains neutral with regard to jurisdictional claims in published maps and institutional affiliations.

Springer Nature or its licensor (e.g. a society or other partner) holds exclusive rights to this article under a publishing agreement with the author(s) or other rightsholder(s); author self-archiving of the accepted manuscript version of this article is solely governed by the terms of such publishing agreement and applicable law.